




Distinctive Optical Properties of Hierarchically Ordered Nanostructures Self-Assembled from Multiblock Copolymer/Nanoparticle Mixtures

Zaojin Liu, Zhanwen Xu,* Liquan Wang, and Jiaping Lin*

Hybrid materials with hierarchical nanostructures are of great interest for their advanced functions. However, the effect of the formation of hierarchical nanostructures on properties is not well understood. Here, through combining dissipative particle dynamics simulation and the finite-difference time-domain method, the optical properties of hierarchically ordered nanostructures formed by mixtures of $A(BC)_n$ multiblock copolymers and nanoparticles (NPs) are investigated. A series of hierarchically ordered nanostructures with multiple small-length-scale hybrid domains are obtained from the self-assembly of $A(BC)_n/$ NP. An increase and blueshift in optical absorption are observed when the number of small-length-scale hybrid domains increases. The small-length-scale hybrid domains enhance light scattering, which consequently contributes to the improved optical performance. These findings can yield guidelines for designing hierarchically ordered functional nanocomposites with light-harvesting characteristics.

Hybrid hierarchical nanostructures can be observed in nature such as bone, shell, attachment pads of geckos, and butterflies' wings.^[1–4] In these hierarchical nanostructures, each constituent at different length scales exhibits its characteristic features, which leads to the complexity and variations of the enhanced macroscopic properties such as high toughness and distinctive optical properties. For example, length-scales of black butterflies' wings exhibit a wide variety of hierarchical micro- and nanostructures with specific functionalities such as visual appearance and thermoregulation.^[5–8] The blackness of these butterfly wings is attributed to the hierarchical nanostructures, which play an important role in harvesting incoming light. For these reasons, mimicking the nature to design and fabricate hierarchically ordered nanostructures is of great interest from both theoretical and engineering viewpoints.

Z. Liu, Dr. Z. Xu, Dr. L. Wang, Prof. J. Lin
Shanghai Key Laboratory of Advanced Polymeric Materials
Key Laboratory for Ultrafine Materials of Ministry of Education
School of Materials Science and Engineering
East China University of Science and Technology
Shanghai 200237, China
E-mail: xuzhanwen0903@126.com; jlin@ecust.edu.cn

 The ORCID identification number(s) for the author(s) of this article can be found under <https://doi.org/10.1002/marc.202000131>.

DOI: 10.1002/marc.202000131

For design of the hierarchical hybrid nanostructures, block polymer/nanoparticle mixtures are particularly attractive.^[9–12] As a typical kind of block copolymers, the linear multiblock copolymers such as $A-b-(B-b-C)_m-b-B-b-A$ and $A(BC)_n$ multiblock copolymers can self-assemble into a variety of hierarchically ordered nanostructures, which are ideal templates to direct the organization of nanoparticles.^[13,14] For example, Zhang and Lin have predicted hierarchical hybrid nanostructures in the mixture of block copolymer/nanoparticle by using self-consistent field and density function theories.^[15] They found that the hierarchical organization of nanoparticles within the ordered structures depends on the particle concentration and particle radius, which lays a foundation for preparing hierarchical hybrid materials with advanced functional properties such as optical properties. The mechanical and photovoltaic properties of hierarchical ordered nanostructures have been predicted to be significantly improved than the normal structures.^[16,17] A further study on the optical absorption properties of the hierarchically ordered hybrid nanostructures is desired, which could facilitate the design of optoelectronic devices with enhanced optical performance.

The correlation between the self-assembled structures and the optical properties in the hybrid self-assembled systems can be revealed by using theoretical simulation approaches. A number of simulation methods, including self-consistent field theory/density functional theory (SCFT/DFT),^[15] molecular dynamics,^[18,19] and dissipative particle dynamics (DPD),^[20] have been proposed to investigate the self-assembly of the mixture of copolymers and nanoparticles. For evaluation of the optical properties, the finite-difference time-domain (FDTD) method is widely used.^[6,21,22] For example, Buxton et al. combined SCFT and DFT to determine the nanostructures of the diblock copolymer/nanoparticle mixtures, and then applied FDTD to investigate the relationship between the nanostructures and optical properties.^[23] It was found that the spatial distribution of particles significantly affected the frequency of reflection. Yan and co-workers applied DPD and FDTD simulations to determine the relationship between the interfacial nanostructures and the optical response for block copolymer/Janus nanoparticle mixtures.^[24] They found that the band gaps and principal

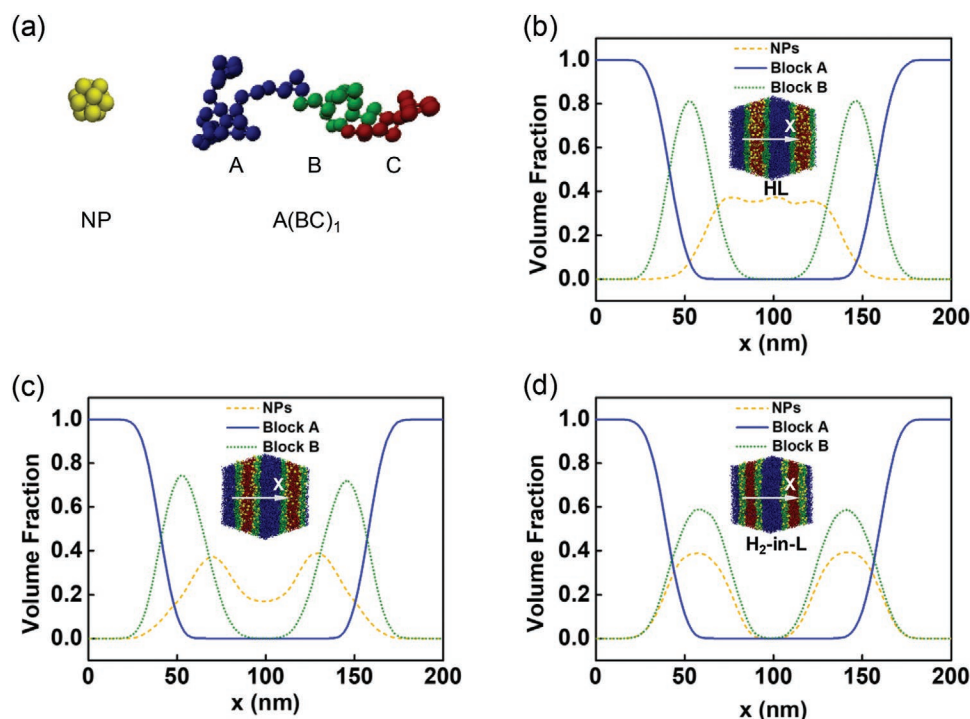


Figure 1. a) The model of the nanoparticles and $A(BC)_1$ multiblock copolymers. b–d) 1D density profiles along the x -arrow for the distribution of nanoparticles (yellow dashed line), A blocks (blue solid line), and B blocks (green dotted line) in the $A(BC)_1$ /NP mixtures at various a_{CN} values: b) $a_{CN} = 15$, c) $a_{CN} = 20$, and d) $a_{CN} = 40$.

frequency depend on the nanoparticle distributions that can be modulated through tuning the stiffness of the semiflexible polymer. The success of the combination of simulation techniques makes it ready to be extended to examine the optical properties of hierarchically ordered nanostructures consisting of multiblock copolymers and nanoparticles.

It has been found that various copolymer systems (e.g., $A(BC)_n$ multiblock copolymer) self-assemble into hierarchically ordered nanostructures that can serve as template for the organization of nanoparticles.^[14] Herein, we systematically explore the optical properties of the hierarchically ordered nanostructures involving the $A(BC)_n$ multiblock copolymers and nanoparticles via theoretical simulations. In the simulations, DPD was applied to study the morphology of the $A(BC)_n$ /nanoparticle system, and subsequently FDTD was utilized to calculate the optical properties of the self-assembled nanostructures. A series of lamellae-in-lamellar hybrid hierarchical nanostructures self-assembled from $A(BC)_n$ /nanoparticle were predicted through DPD simulations. The hierarchically ordered distribution of nanoparticles results in a marked improvement and blueshift in optical absorption. We expect that these findings can help understand the effect of the formation of the hierarchical ordered nanostructures on the optical properties of block copolymer/nanoparticle mixtures and provide guidance for designing advanced functional nanocomposites with enhanced optical performance.

The following paragraphs present a study on the self-assembled nanostructures and optical properties of the $A(BC)_n$ /NP mixtures. First, we studied the effect of the interaction parameters and the number of repeat BC units on the self-assembled

nanostructures of the $A(BC)_n$ /NP mixtures. Then, we focused on the optical properties of these self-assembled nanostructures. The dielectric parameters including the dielectric constants of the polymers and nanoparticles were tuned to examine the generality of our findings. Last, a comparison between the simulation results and experimental evidences was made.

In the $A(BC)_n$ multiblock copolymer/nanoparticle mixtures, the multiblock copolymers can self-assemble into hierarchically ordered nanostructures. In addition, the distribution of nanoparticles in the self-assembled structures can be modulated by regulating the architecture of the $A(BC)_n$ multiblock copolymer (i.e., the number of repeat BC units n) or the surface chemistry of the nanoparticles (i.e., the interaction strength between the blocks and nanoparticles).^[25] To understand the dependence of nanoparticle distribution in $A(BC)_n$ multiblock copolymers on the architecture of the copolymer and the interaction parameters, we carried out simulations of the mixture systems with various values of the interaction parameters and n .

We first studied the effect of the interaction parameter between C blocks and nanoparticles a_{CN} on the self-assembled nanostructures of the $A(BC)_1$ /NP mixtures. **Figure 1b–d** shows the 1D density profiles of the nanoparticles, A blocks and B blocks in the self-assembled nanostructures of $A(BC)_1$ /NP at various a_{CN} . As shown in Figure 1b, the $A(BC)_1$ copolymers form a parallel lamellae-in-lamellar hierarchical structure, which serves as a template to direct the distribution of nanoparticles. As the nanoparticles are selective to C blocks ($a_{CN} = 15$, which is smaller than the a_{BN}), the nanoparticles are distributed into the C domains between two adjacent B domains, forming a C/N hybrid domain. We name this structure as HL. In the

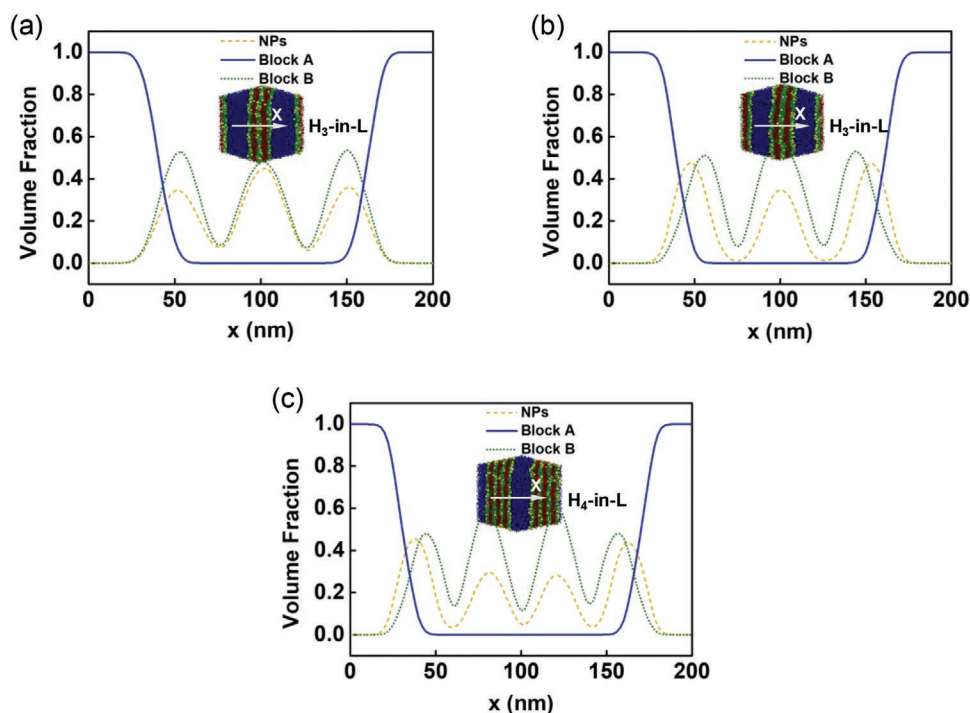


Figure 2. 1D density profiles along the x -arrow for the distribution of nanoparticles (yellow dashed line), A blocks (blue solid line), and B blocks (green dotted line) in a) $A(BC)_2/NP$, b) $A(BC)_3/NP$, and c) $A(BC)_4/NP$ at $a_{CN} = 40$.

HL, the nanoparticle distribution is single-periodic. When the a_{CN} increases to the value equal to the a_{BN} , the nanoparticles are distributed into both B and C domains, as can be seen from Figure 1c. It is noted that an interfacial segregation of nanoparticles occurs at the interface between B and C domains. In this case, the segregation of the nanoparticles at the interface could contribute to the reduction of the interface energy between B and C blocks.^[15] At a higher repulsive parameter a_{CN} , due to the higher repulsion between nanoparticles and C blocks, the nanoparticles are selective to B blocks. As shown in Figure 1d, the nanoparticles selective to B blocks are mainly distributed into B domains forming B/N hybrid domains. The hierarchical lamellar structure with two B/N hybrid domains between every two neighboring A domains is formed. The size of these hybrid domains is much smaller than that of A domains. This structure is named as H_2 -in-L. In the H_2 -in-L, the nanoparticle distribution is double-periodic.

Then, we studied the influence of the number of BC repeat units n on the self-assembled nanostructures of $A(BC)_n/NP$ mixtures. The nanoparticles with B block selectiveness are considered, which can result in the formation of B/N hybrid domains (Figure 1d). **Figure 2a–c** shows the 1D density profiles of the nanoparticles, A blocks and B blocks in the $A(BC)_n/NP$ mixtures with various n . As can be seen from Figure 2a,b, the B and C blocks in the $A(BC)_2/NP$ and $A(BC)_3/NP$ mixtures separate into three B small-length-scale domains and two C small-length-scale domains between every two neighboring A domains, respectively. The nanoparticles are distributed into the B domains, forming three B/N hybrid domains between every two neighboring A domains. We name these structures as H_3 -in-L, in which the nanoparticle distribution is also

double-periodic. As $A(BC)_4$ has one more short BC repeat unit than $A(BC)_3$, one more small-length-scale B/N hybrid domains are formed between every two neighboring large A domains in $A(BC)_4/NP$ mixtures (H_4 -in-L, see Figure 2c). It should be noted that when the nanoparticles are selective to C blocks, small-length-scale C/N hybrid domains are formed and the number of C/N hybrid domains increases with increasing number of BC repeat units (see Figure S2, Supporting Information).

The correlation between the optical properties and hybrid hierarchical nanostructures was explored. We employed FDTD simulations to examine the optical properties of the hierarchical hybrid nanostructures. The schematic presentation of the computational domain used for FDTD simulations is shown in **Figure 3a**. In the FDTD simulations, a broadband (wavelength 300–700 nm) plane wave with transverse magnetic (TM) polarization (electric field E_z perpendicular to the x - y plane) was applied. Two monitors were placed above and below the self-assembled nanostructure to measure reflection ($R(\lambda)$) and transmission strength ($T(\lambda)$), respectively. Then, the frequency-dependent optical absorption can be calculated with $A(\lambda) = 1 - T(\lambda) - R(\lambda)$.

Figure 3b shows the absorption spectra of the self-assembled nanostructures of the $A(BC)_1/NP$ under the plane wave with a normal angle of incidence (AOI). As can be seen, the optical absorption increases with increasing a_{CN} in the entire visible spectrum (300–700 nm). With increasing a_{CN} , the self-assembled nanostructures undergo the transformation from the HL into the hierarchical hybrid H_2 -in-L (see Figure 1b–d). The increase in the optical absorption means that the formation of the H_2 -in-L improves the optical performance. To show the advantages of the H_2 -in-L structures in optical absorption,

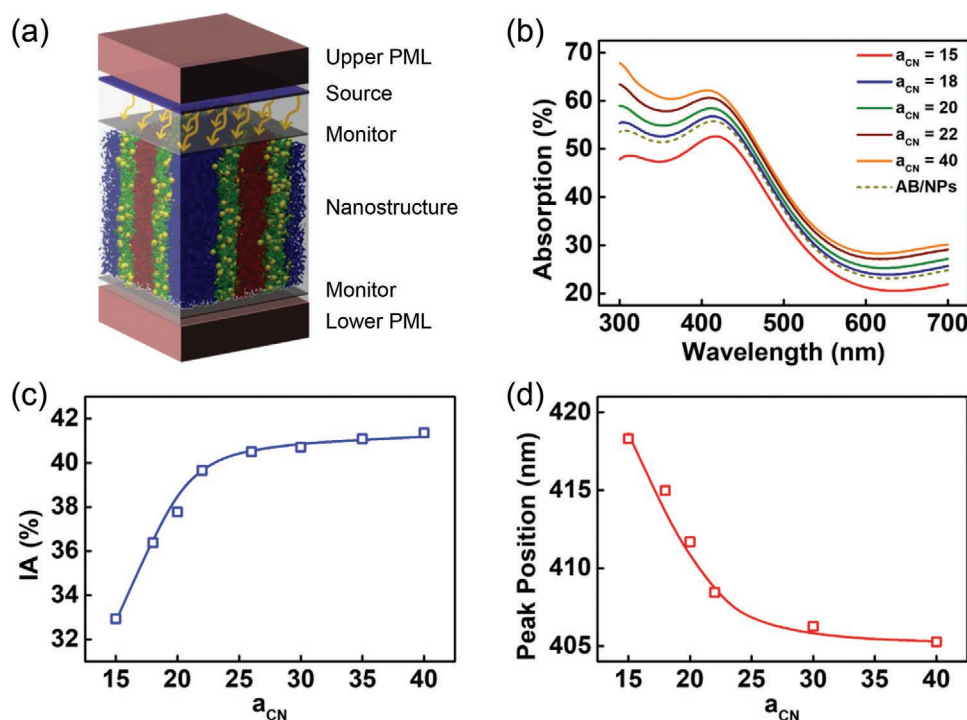


Figure 3. a) Schematic illustration of the computational domain used in the FDTD simulations. b) The solid lines are the optical absorption spectra of $A(BC)_1/$ NP mixtures at various a_{CN} . The dashed line is the optical absorption spectrum of the AB/NP mixture with a general lamellar structure. c) Plot of IA of $A(BC)_1/$ NP mixtures as a function of the repulsive parameter a_{CN} . d) Plot of the wavelength of absorption peak of $A(BC)_1/$ NP mixtures as a function of a_{CN} .

we also calculated the optical properties of the general lamellar nanostructure of AB diblock copolymer/NP mixtures for a comparison. The length of the A and B blocks in the diblock copolymer was set to be equal to that of the long block of the $A(BC)_n$ multiblock copolymers. The nanoparticles were set to be selective to the B blocks. In the AB diblock copolymer/NP mixture, the AB diblock copolymers self-assemble into a general lamellar nanostructure and the nanoparticles are distributed into B domains, forming a general hybrid lamellar nanostructure with B/N hybrid domains (see Figure S3, Supporting Information). From Figure 3b, it can be seen that the optical absorption of the general hybrid lamellar nanostructure is lower than that of the H_2 -in-L structure. It should be noted that the nanoparticle distribution in both the HL and general hybrid lamellae is single-periodic. The higher optical absorption of the H_2 -in-L than both of these two structures means that the formation of double-periodic distribution of nanoparticles in the $A(BC)_n/$ NP can lead to improved optical performance.

To assess the light-absorbing capability of the self-assembled nanostructures of $A(BC)_1/$ NP mixtures, the integrated absorption (IA) over the band from 300 to 700 nm was calculated and plotted in Figure 3c. With increasing a_{CN} , the IA first increases markedly and then remains almost unchanged with the formation of two small-length-scale hybrid domains. The IA of H_2 -in-L is significantly higher than the HL structure. From Figure 3b, it can be also seen that the wavelength and width of the absorption peak are influenced by the self-assembled nanostructures. Compared with the HL, the absorption peak of H_2 -in-L covers a larger bandwidth. Figure 3d shows the wave length of

absorption peak as a function of a_{CN} . The wavelength of absorption peak decreases with increasing a_{CN} , as the nanostructures undergo the transformation from HL to H_2 -in-L. Since a smaller periodic grating nanostructures result in a shorter wavelength of absorption peak,^[26,27] the blueshift of the absorption peak can be attributed to the formation of the small-length-scale hybrid domains with double-periodic nanoparticle distribution.

To understand the physical mechanisms of the significant difference in optical absorption between the HL and H_2 -in-L nanostructures, we analyzed the distributions of magnetic field (H_y) and power absorption in these two nanostructures under the illumination with three different wavelengths of 350, 450, and 600 nm. It can be seen from Figure 4a that most magnetic field are confined in the polymer domains of these self-assembled nanostructures. Additionally, the magnetic field near the interface between pure polymer domains and hybrid domains is much higher than that of the other regions. Significant differences are observed in the magnetic field distribution between the HL and H_2 -in-L nanostructures. The area of strong magnetic field in the H_2 -in-L nanostructures is much larger than that of HL, which means that stronger confinement is in the H_2 -in-L nanostructures. The stronger confinement leads stronger light scattering, which results in a wider region of higher power absorption area. As can be seen in Figure 4b, for all the wavelengths of 350, 450, and 600 nm, the power absorption in the H_2 -in-L is much stronger and wider than that in the HL nanostructures.

Since the incident angle was crucial for photovoltaic device performance at different times of a day, we then examined the

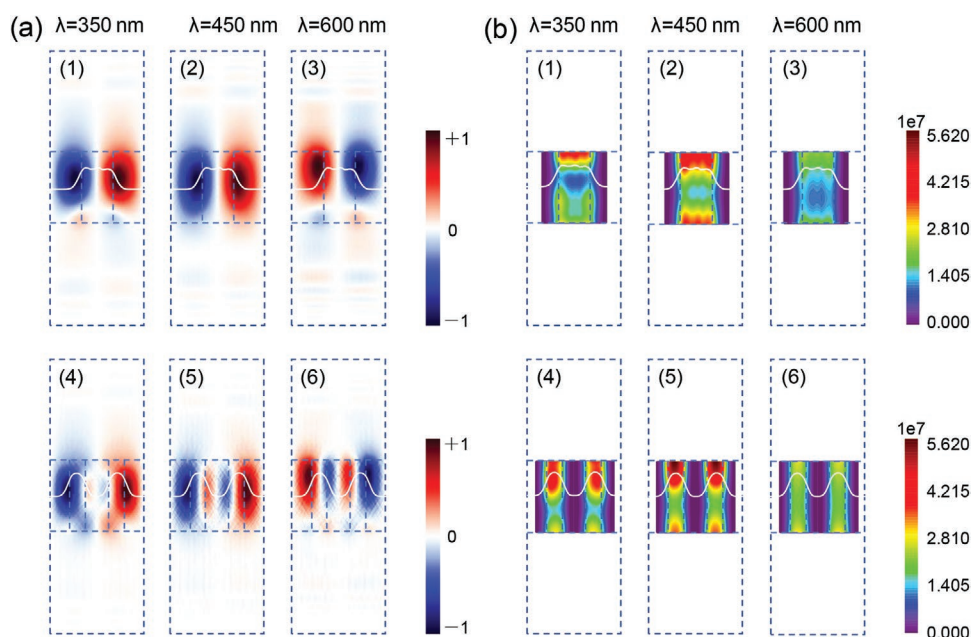


Figure 4. a) Spatial distribution of the y -component magnetic field (H_y) for the hybrid nanostructures HL (1–3) and H_2 -in-L (4–6) at three different TM wave λ under normal incidence. The colors range from blue (negative magnetic field) to red (positive magnetic field). b) 2D absorbed power map for the hybrid nanostructures HL (1–3) and H_2 -in-L (4–6) at three different TM wave λ . The colors range from blue (weaker absorption) to red (stronger absorption). The white line represents the nanoparticle density in the HL and H_2 -in-L.

influence of the incident angle on the absorption efficiency of the hybrid hierarchical nanostructures. **Figure 5a,b** shows the contour plot of the absorption values in the plane of the wavelength and AOI in the HL and H_2 -in-L. As can be seen, when

the wavelength of the incident light is below 500 nm, the light absorption changes slightly with increasing AOI. As the wavelength gets above 500 nm, the optical absorptions of both nanostructures decrease significantly with increasing AOI. A picture

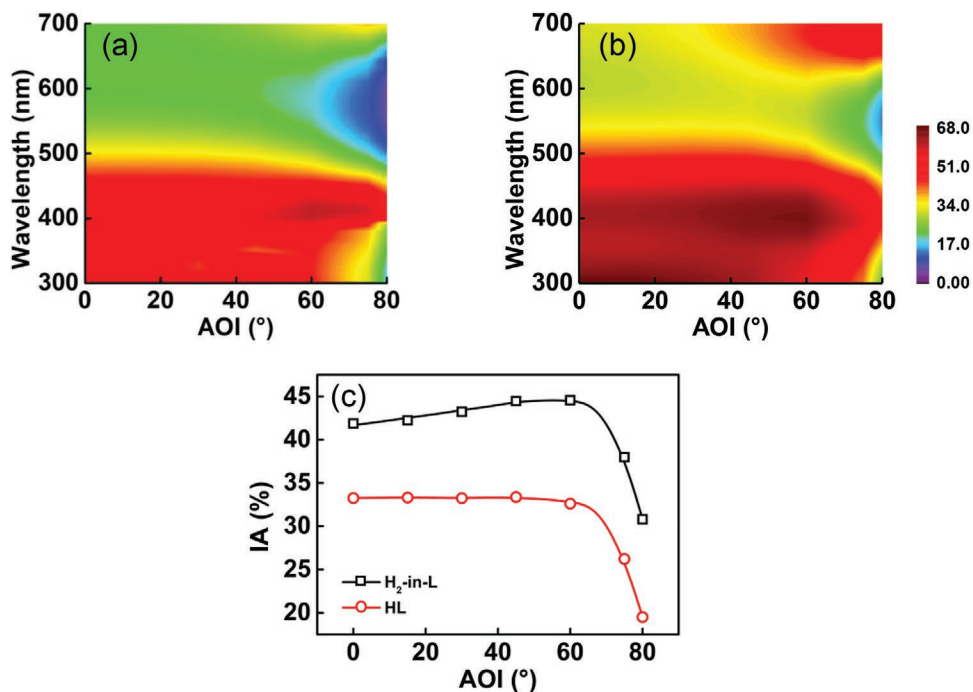


Figure 5. a,b) The contour plot of the absorption values in the plane of the wavelength and AOI in the hybrid nanostructures: a) HL and b) H_2 -in-L. The colors range from blue (weaker absorption) to red (stronger absorption). c) Plot of IA as a function of AOI in H_2 -in-L (black solid line) and HL (red solid line).

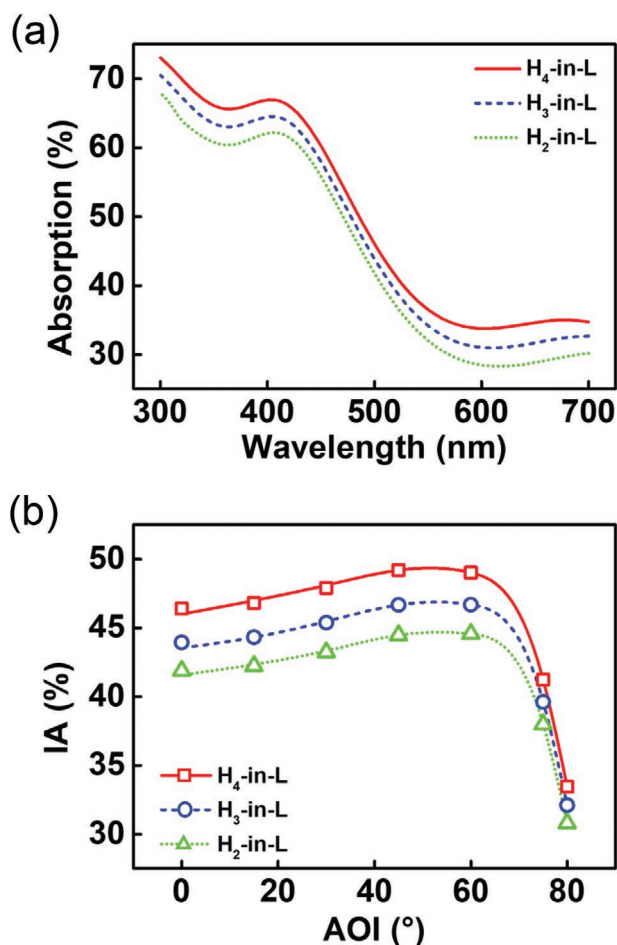


Figure 6. a) Optical absorption spectra of the hierarchical nanostructures with various number of small-length-scale hybrid domains: H₄-in-L (red solid line), H₃-in-L (blue dashed line), and H₂-in-L (green dotted line). b) Plot of IA as a function of AOI of H₄-in-L (red solid line), H₃-in-L (blue dashed line), and H₂-in-L (green dotted line).

exhibiting the sensitivity of the optical absorption to AOI can be obtained by calculating the IA at various AOI (see Figure 5c). As can be seen, the optical absorption of H₂-in-L nanostructure is always higher than that of HL nanostructure at various AOI. Additionally, we investigated the effect of the polarization of the incident light on optical absorption of the hybrid nanostructures. As shown in Figure S4, Supporting Information, for the transverse electric (TE) polarization, the absorption value of the HL nanostructure is significantly lower than that of the H₂-in-L nanostructure at various AOI. These results indicate that the optical absorption of the H₂-in-L is higher than that of the HL for both TM and TE modes at a wide range of AOI.

To examine the effect of the number of small-length-scale hybrid domains on optical absorption, we calculated the optical absorption of H₃-in-L and H₄-in-L. **Figure 6a** displays the optical absorption performance of these nanostructures as a function of the wavelength in the range of 300–700 nm for a plane wave with a normal AOI. It can be seen that the optical absorption increases with increasing number of small-length-scale hybrid domains in the entire range of optical wavelength. Additionally, the peaks of the absorption spectrum exhibit a blue-shift

as the number of small-length-scale hybrid domains increases. Note that in the case of the A(BC)_n/NP mixtures with the nanoparticle selective to C blocks, we also observed the increase and blueshift in optical absorption as the number of small-length-scale C/N hybrid domains increases (see Figure S5, Supporting Information). Influence of the AOI on the IA in the H₃-in-L and H₄-in-L nanostructures is also investigated (see Figure 6b). When the AOI is less than 60°, the IA of these nanostructures increases slightly with increasing AOI. When the AOI is greater than 60°, the IA decreases dramatically with increasing AOI due to the significantly enhanced reflection of the incident light (see Figure S6, Supporting Information). Notably, among these nanostructures, the H₄-in-L with the largest number of small-length-scale hybrid domains always exhibits the highest optical absorption within the whole range of AOI.

The above theoretical simulations show that the optical absorption of the A(BC)_n/NP mixtures can be improved when the nanostructures evolve from the HL with single-periodic nanoparticle distribution to the H-in-L with multiple small-length-scale hybrid domains. To confirm the generality of our findings, we investigated the effect of some important dielectric parameters on the optical properties of hierarchical hybrid nanostructures, including dielectric constants of the copolymers and nanoparticles. The effect of the dielectric constants of the polymers was first investigated. We increased the dielectric constants of polymer from 1.5 to 5.0, which covers the range of dielectric constants of typical polymeric materials.^[28,29] The light absorption decreases with increasing dielectric constants of polymers, as shown in **Figure 7**. Polymers with a higher dielectric constants can enhance reflection,^[30] resulting in the decrease of light absorption. The IA of the H-in-L nanostructures keeps higher than that of the HL nanostructures as the dielectric constants of polymers increase. Additionally, for the H-in-L nanostructures, the optical absorption increases as the number of the small hybrid domains increases.

The effect of the types of nanoparticles on the optical absorption of the hybrid nanostructures was also studied. Four kinds of metal nanoparticle commonly used in optoelectronic devices (including Ag, Pt, Ni, and Ti) were considered. The dielectric parameters of these metals were taken from the literatures.^[31–35] **Figure 8a–d** shows the absorption spectra of the self-assembled hybrid nanostructures with these kinds of nanoparticles. In the range of 300–700 nm, the optical absorption of the H-in-L is always higher than that of the HL. As a result, the H-in-L nanostructures exhibit a significant IA improvement in comparison with the HL nanostructure. In particular, the IA of H₂-in-L nanostructure is around 50% higher than that of HL nanostructure for Ag nanoparticle. For the other three kinds of nanoparticles, the enhancement of IA exceeds about 10% when the self-assembled structures change from the HL to H₂-in-L. Additionally, for all these kinds of nanoparticles, the IA of these hierarchical nanostructures is found to increase with increasing number of small-length-scale hybrid domains (see Figure S7, Supporting Information).

To the best of our knowledge, there is no experimental study on the optical properties of the hierarchical nanostructures self-assembled from multiblock copolymer/nanoparticle mixtures. Therefore, it is difficult to make direct comparisons between the experimental observations and the theoretical predictions.

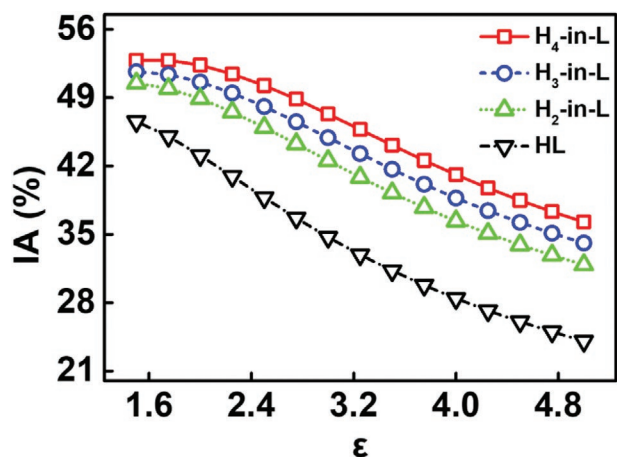


Figure 7. Plot of IA as a function of the dielectric constants of the polymer components for H_4 -in-L (red solid line), H_3 -in-L (blue dash line), H_2 -in-L (green dotted line), and HL (black dashed dotted line).

However, there exist some experimental evidences regarding the self-assembled nanostructures and optical properties of diblock copolymer/nanoparticle mixtures,^[10,36–38] which support the simulation results of the optical properties of the multiblock copolymer/nanoparticle mixtures. For instance, Thomas and co-workers have investigated the hybrid lamellar structures and optical properties of the poly(styrene-*b*-ethylene propylene) copolymer (PS-*b*-PEP)/gold nanoparticle mixtures.^[36] Two types of hybrid lamellar structures were obtained through tuning the surface chemistry of gold nanoparticles: nanoparticles confined at the interfacial areas and nanoparticles dispersed uniformly

within the selective polymer domains. They found that the confinement of nanoparticles at the interfacial areas led to an obvious increase in optical absorption.

In the simulations, the nanoparticle distribution was modulated through tuning the interaction parameter between nanoparticles and C blocks a_{CN} , corresponding to the change in the surface chemistry of nanoparticles. With increasing a_{CN} , the nanostructures transform from the one with nanoparticles dispersing uniformly in the C domains (Figure 1b) to the one with nanoparticles concentrating at the interfacial area between B and C domains (Figure 1c). This gives rise to an increase in optical absorption (see Figure 3b). This result is qualitatively consistent with the experimental observations from Thomas and co-workers. The qualitative consistency between the experimental observations and the theoretical predictions confirms the effects of nanoparticle distribution on the optical performance of the copolymer/nanoparticle mixtures.

Beyond reproducing some phenomenon observed in the experimental work, we propose a new strategy of using multiblock copolymer/nanoparticle mixtures to improve the optical absorption. Through tuning the a_{CN} or molecular design of multiblock copolymer, a series of hierarchically ordered hybrid nanostructures with multiple small-length-scale hybrid domains can be obtained. The simulation results demonstrate that the formation of the multiple small-length-scale hybrid domains with double-periodic nanoparticle distribution results in an increase and blueshift in optical absorption. Because these structural characteristics of the hierarchical hybrid nanostructures are achievable in molecular design of multiblock copolymers and can be controlled via the surface modification of nanoparticles, mixing the multiblock copolymers

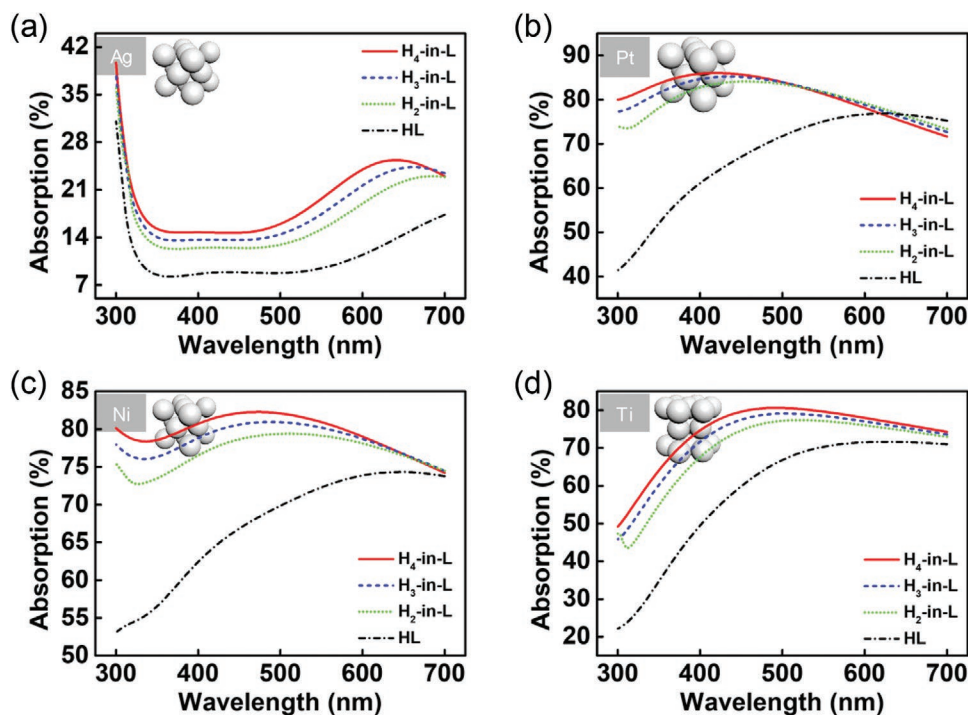


Figure 8. Optical absorption spectra of the hierarchical nanostructures with different kinds of nanoparticles: a) Ag, b) Pt, c) Ni, and d) Ti. The red solid line, blue dashed line, green dotted line and black dashed dotted line represent the H_4 -in-L, H_3 -in-L, H_2 -in-L, and HL, respectively.

and nanoparticles can be a promising strategy for fabricating advanced functional nanocomposites with improved optical performance. For example, the multiblock copolymer/nanoparticle mixtures can be applied in polymer solar cells to enhance the light absorption and improve the photovoltaic performance. The weak optical absorption of block copolymer based polymer solar cells is the critical reason for its low efficiency. According to our theoretical predictions, embedding nanoparticles into the active layers of block copolymer-based polymer solar cells and making the nanoparticle distribution hierarchically ordered can help them harvest more light and level up the photovoltaic performance.

In summary, we coupled DPD simulation with FDTD to investigate the optical absorption of hierarchically ordered nanostructures self-assembled from the mixtures of A(BC)_n multiblock copolymers and nanoparticles. The nanoparticle distribution in the self-assembled nanostructures was modulated via regulating the molecular architectures and interaction parameters between the nanoparticles and copolymers. Hierarchically ordered nanostructures with multiple small-length-scale hybrid domains were obtained. The small-length-scale hybrid domains in the hierarchically ordered nanostructures give rise to the enhancement and blueshift in optical absorption. The increase in optical absorption is mainly due to the enhancement in light confinement and scattering in the hybrid hierarchical nanostructures. These findings could provide useful information for designing and preparing advanced functional materials such as light-harvesting systems.

Experimental Section

To investigate the relationship between the self-assembled nanostructures and the optical properties of the multiblock copolymer/nanoparticle mixtures, we combined DPD for self-assembled morphological studies and FDTD for optical property calculations.

DPD, a mesoscopic simulation method, is widely used to investigate the copolymer self-assembly.^[39,40] In the DPD method, a coarse graining bead (DPD bead) represents a clustering group of atoms. The evolution of DPD beads is described by Newton's equations of motion

$$\frac{d\mathbf{r}_i}{dt} = \mathbf{v}_i, m_i \frac{d\mathbf{v}_i}{dt} = \mathbf{f}_i \quad (1)$$

where t is the time and m_i is the mass of the i th bead. \mathbf{r}_i , \mathbf{v}_i , and \mathbf{f}_i denote the position, velocity, and total force of the i th bead, respectively. The force acting on a i th bead, \mathbf{f}_i , consists of three parts, for example, the conservative force (\mathbf{F}_{ij}^C), the dissipative force (\mathbf{F}_{ij}^D), and the random force (\mathbf{F}_{ij}^R). The sum of the three interactions is given by

$$\mathbf{f}_i = \sum_{j \neq i} (\mathbf{F}_{ij}^C + \mathbf{F}_{ij}^D + \mathbf{F}_{ij}^R) \quad (2)$$

In the DPD simulations, coarse-grained models of A(BC)_n multiblock copolymers and nanoparticles were constructed, as illustrated in Figure 1a. The multiblock copolymers consist of long A blocks and short BC blocks. The A(BC)_n multiblock copolymers contained 60 DPD beads. The volume fraction of A block was fixed at 0.5, and the ratio of B block to C block was 1:1. The n represents the number of BC blocks, which varied from 1 to 4. Each nanoparticle contains 13 beads with one bead in the center and 12 around. The volume fraction of nanoparticle was fixed at 0.15. The interaction strengths a_{ij} between DPD beads of same types were given by $a_{AA} = a_{BB} = a_{CC} = a_{NN} = 25$, where A, B, C,

and N represent the beads in the A blocks, B blocks, C blocks, and nanoparticles, respectively. The interaction parameters between different kind of blocks were set as $a_{AB} = a_{AC} = 70$ and $a_{BC} = 75$. We examined the case where nanoparticles were attracted by B block ($a_{BN} = 20$) and the repulsive interaction parameter between nanoparticle and C block a_{CN} was varied from 15 to 40. The DPD simulation under NVT ensemble was performed in $30 \times 30 \times 30$ cubic box with periodic boundary conditions. The density of system was set to be 3. All of the nanostructures were obtained after DPD simulation was carried out for at least 1×10^7 steps. This can ensure the equilibrium states of the systems.^[41] Details of the DPD method can be found in Supporting Information (see Section 1 of the Supporting Information).

Once we had determined the structures self-assembled from the multiblock copolymer/nanoparticle mixtures, the FDTD was used to model the propagation of light through the mixtures. The FDTD proposed by Yee is a methodology for numerically solving Maxwell's equation.^[42] The local dielectric constants of the media in the FDTD simulation can be obtained by linearly weighting the contributions of the different components

$$\varepsilon(\mathbf{r}) = \phi_A(\mathbf{r})\varepsilon_A + \phi_B(\mathbf{r})\varepsilon_B + \phi_C(\mathbf{r})\varepsilon_C + \phi_{NP}(\mathbf{r})\varepsilon_{NP} \quad (3)$$

where ε_i denotes the dielectric constants of component i , and $\phi_i(\mathbf{r})$ characterizes the volume fraction of component i at \mathbf{r} .^[23,43] In this work, the nanoparticles were set to be optical active materials while the polymers were set to be incapable of absorbing light. The dielectric constant of each block in multiblock was set to be the typical values of polymeric materials.^[44] The nanoparticles were set as gold nanoparticles. The complex optical constants of the gold nanoparticles can be described by the Lorentz dispersion model, given by^[31]

$$\varepsilon_r = \varepsilon_\infty + \sum_j \frac{\sigma_j \omega_j^2}{\omega_j^2 - \omega^2 - i\omega\gamma_j} \quad (4)$$

where ω is the frequency of incident light and ε_∞ is the dielectric constant corresponding to the infinite frequency. ω_j , γ_j , and σ_j denote the resonance frequency, the damping coefficient, and the oscillator strength, respectively. The values of these parameters used in this work are shown in Table S1, Supporting Information.

The FDTD simulations were performed using a software package, known as Meep, developed at MIT.^[45] In Meep, the resolution was set as 500 Yee cells per unit length, corresponding to an effective spatial resolution of 2 nm. The thickness of the unit cell was set as 200 nm. The boundary conditions of the computing unit cell were set as periodical and two perfect matching layers (PML) were put at both ends in the unit cell. A broadband (wavelength 300–700 nm) plane wave source was placed above the upper surface of the self-assembled hybrid nanostructures. Two power monitors were placed in front of the two PML of the unit cell to measure both the transmission spectra ($T(\lambda)$) and reflection spectra ($R(\lambda)$) and the absorption spectra is calculated by^[46]

$$A(\lambda) = 1 - T(\lambda) - R(\lambda) \quad (5)$$

To quantify the broadband absorption within the entire wavelength spectrum (300–700 nm), the IA is calculated by^[47]

$$IA = \frac{\int_{300}^{700} A(\lambda) \frac{dI}{d\lambda} d\lambda}{\int_{300}^{700} \frac{dI}{d\lambda} d\lambda} \quad (6)$$

where $\frac{dI}{d\lambda}$ is the incident solar radiation intensity per unit wavelength that was obtained from the spectral irradiance of the sun (<http://rredc.nrel.gov/solar/spectra/am1.5/>, American Society for Testing and Materials, AM1.5 standard curve). The details of discretization forms of Maxwell's

equations on the Yee cells can be found in Supporting Information (see Section 2 of the Supporting Information).

Supporting Information

Supporting Information is available from the Wiley Online Library or from the author.

Acknowledgements

This work was supported by the National Natural Science Foundation of China (51833003, 51621002, and 21975073).

Conflict of Interest

The authors declare no conflict of interest.

Keywords

multiblock copolymers, nanoparticles, nanostructures, optical properties, self-assembly

Received: March 11, 2020
Published online: April 24, 2020

- [1] P. Fratzl, R. Weinkamer, *Prog. Mater. Sci.* **2007**, *52*, 1263.
 [2] H. D. Espinosa, J. E. Rim, F. Barthelat, M. J. Buehler, *Prog. Mater. Sci.* **2009**, *54*, 1059.
 [3] K. Autumn, Y. A. Liang, S. T. Hsieh, W. Zesch, W. P. Chan, T. W. Kenny, R. Fearing, R. J. Full, *Nature* **2000**, *405*, 681.
 [4] H. Butt, A. K. Yetisen, D. Mistry, S. A. Khan, M. U. Hassan, S. H. Yun, *Adv. Opt. Mater.* **2016**, *4*, 497.
 [5] P. Vukusic, J. R. Sambles, C. R. Lawrence, *Proc. R. Soc. London, Ser. B* **2004**, *271*, S237.
 [6] Q. Zhao, X. Guo, T. Fan, J. Ding, D. Zhang, Q. Guo, *Soft Matter* **2011**, *7*, 11433.
 [7] R. E. Rodriguez, S. P. Agarwal, S. An, E. Kazyak, D. Das, W. Shang, R. Skye, T. Deng, N. P. Dasgupta, *ACS Appl. Mater. Interfaces* **2018**, *10*, 4614.
 [8] A. D. Pris, Y. Utturkar, C. Surman, W. G. Morris, A. Vert, S. Zalyubovskiy, T. Deng, H. T. Ghiradella, R. A. Potyrailo, *Nat. Photonics* **2012**, *6*, 195.
 [9] W. A. Lopes, H. M. Jaeger, *Nature* **2001**, *414*, 735.
 [10] M. R. Bockstaller, R. A. Mickiewicz, E. L. Thomas, *Adv. Mater.* **2005**, *17*, 1331.
 [11] H. Kang, F. A. Detcheverry, A. N. Mangham, M. P. Stoykovich, K. Daoulas, R. J. Hamers, M. Müller, J. J. de Pablo, P. F. Nealey, *Phys. Rev. Lett.* **2008**, *100*, 148303.
 [12] D.-P. Song, C. Li, N. S. Colella, X. Lu, J.-H. Lee, J. J. Watkins, *Adv. Opt. Mater.* **2015**, *3*, 1169.
 [13] A. Subbotin, T. Klymko, G. ten Brinke, *Macromolecules* **2007**, *40*, 2915.
 [14] L. Wang, J. Lin, L. Zhang, *Macromolecules* **2010**, *43*, 1602.
 [15] L. Zhang, J. Lin, *Macromolecules* **2009**, *42*, 1410.
 [16] X. Zhu, L. Wang, J. Lin, *Macromolecules* **2011**, *44*, 8314.
 [17] Z. Xu, J. Lin, L. Zhang, L. Wang, G. Wang, X. Tian, T. Jiang, *ACS Appl. Mater. Interfaces* **2018**, *10*, 22552.
 [18] L. Wang, H. Liu, F. Li, J. Shen, Z. Zheng, Y. Gao, J. Liu, Y. Wu, L. Zhang, *Phys. Chem. Chem. Phys.* **2016**, *18*, 27232.
 [19] P. Xu, J. Lin, L. Zhang, *J. Phys. Chem. C* **2017**, *121*, 28194.
 [20] Q. Li, L. Wang, J. Lin, *Phys. Chem. Chem. Phys.* **2017**, *19*, 24135.
 [21] X. Yang, L. Zhang, M. Yang, S. Niu, H. Song, J. Ni, C. Wu, G. Chen, *Mater. Lett.* **2018**, *221*, 26.
 [22] C. Lundgren, R. Lopez, J. Redwing, K. Melde, *Opt. Express* **2013**, *21*, A392.
 [23] G. A. Buxton, J. Y. Lee, A. C. Balazs, *Macromolecules* **2003**, *36*, 9631.
 [24] B. Dong, Z. Huang, H. Chen, L.-T. Yan, *Macromolecules* **2015**, *48*, 5385.
 [25] Y. Mai, A. Eisenberg, *Acc. Chem. Res.* **2012**, *45*, 1657.
 [26] C. Tan, Z. Yue, Z. Dai, Q. Bao, X. Wang, H. Lu, L. Wang, *Opt. Mater.* **2018**, *86*, 421.
 [27] J. Wu, C. Zhou, J. Yu, H. Cao, S. Li, W. Jia, *Opt. Commun.* **2014**, *329*, 38.
 [28] P. Barber, S. Balasubramanian, Y. Anguchamy, S. Gong, A. Wibowo, H. Gao, H. J. Ploehn, H. C. zur Loye, *Materials* **2009**, *2*, 1697.
 [29] A. Urbas, R. Sharp, Y. Fink, E. L. Thomas, M. Xenidou, L. J. Fetters, *Adv. Mater.* **2000**, *12*, 812.
 [30] S. Walheim, E. Schaffer, J. Mlynek, U. Steiner, *Science* **1999**, *283*, 520.
 [31] A. D. Rakic, A. B. Djurisic, J. M. Elazar, M. L. Majewski, *Appl. Opt.* **1998**, *37*, 5271.
 [32] K. Aydin, V. E. Ferry, R. M. Briggs, H. A. Atwater, *Nat. Commun.* **2011**, *2*, 517.
 [33] X. Li, Z. Wang, Y. Hou, *Opt. Commun.* **2018**, *406*, 95.
 [34] W. Zhang, D. Zhang, T. Fan, J. Gu, J. Ding, H. Wang, Q. Guo, H. Ogawa, *Chem. Mater.* **2009**, *21*, 33.
 [35] Z. Zheng, B. Huang, X. Qin, X. Zhang, Y. Dai, M.-H. Whangbo, *J. Mater. Chem.* **2011**, *21*, 9079.
 [36] M. R. Bockstaller, E. L. Thomas, *Phys. Rev. Lett.* **2004**, *93*, 166106.
 [37] W.-C. Yen, Y.-H. Lee, J.-F. Lin, C.-A. Dai, U.-S. Jeng, W.-F. Su, *Langmuir* **2011**, *27*, 109.
 [38] F. Li, Y. Shi, K. Yuan, Y. Chen, *New J. Chem.* **2013**, *37*, 195.
 [39] Q. Zhang, J. Lin, L. Wang, Z. Xu, *Prog. Polym. Sci.* **2017**, *75*, 1.
 [40] Z. Xu, J. Lin, Q. Zhang, L. Wang, X. Tian, *Polym. Chem.* **2016**, *7*, 3783.
 [41] X. Zhang, L. Wang, L. Zhang, J. Lin, T. Jiang, *Langmuir* **2015**, *31*, 2533.
 [42] K. S. Yee, *IEEE Trans. Antennas Propag.* **1966**, *14*, 302.
 [43] Q. Wang, T. Taniguchi, G. H. Fredrickson, *J. Phys. Chem. B* **2004**, *108*, 6733.
 [44] P. V. K. Thakur, R. K. Gupta, *Chem. Rev.* **2016**, *116*, 4260.
 [45] A. F. Oskooi, D. Roundy, M. Ibanescu, P. Bermel, J. D. Joannopoulos, S. G. Johnson, *Comput. Phys. Commun.* **2010**, *181*, 687.
 [46] L. Zhou, Y. Tan, D. Ji, B. Zhu, P. Zhang, J. Xu, Q. Gan, Z. Yu, J. Zhu, *Sci. Adv.* **2016**, *2*, e1501227.
 [47] Y. J. Donie, M. Smeets, A. Egel, F. Lentz, J. B. Preinfalk, A. Mertens, V. Smirnov, U. Lemmer, K. Bittkau, G. Gomard, *Nanoscale* **2018**, *10*, 6651.